Fast measurements of capillary pressure using the porous plate method: An alternative to MICP

Roland Lenormand*, and *Guillaume* Lenormand

CYDAREX, 130 rue du port Mesquer 44420, France

Abstract. The use of the porous plate method for the measurement of capillary pressure is time consuming, from weeks to months. In this paper we present an apparatus that reduces the duration of such measurements drastically while avoiding the use of toxic mercury. The main applications are the measurements of resistivity index by gas or oil injection, and drainage capillary pressure curves leading to the determination of pore throat size distribution (ptsd), as an alternative to mercury injection (MICP).

Our main improvement was to design an equipment allowing the use of very thin samples (3-6 mm) and the measurement of small effluent volumes. The use of 2 porous plates of the same wettability increases the speed of the production by a factor 2. Using a strong spring instead of a rubber sleeve improves the capillary contact and speed-up the mounting of the equipment. For quality control, the experiment is simulated with the two-phase flow simulator CYDAR to verify that the capillary equilibrium has been reached.

Instead of step injection, it is preferable to use injection with a continuous pressure increase to obtain a smooth Pc curve. With gas injection, capillary pressure curves up to 15 bar were obtained in one day on 6 mm disks with a large range of permeabilities, leading to ptsdt very close to MICP results. This apparatus can be a good alternative to MICP. Since it is fully automatic, less expensive, and easier to operate, several apparatuses can be run in parallel.

Compared to MICP, the main drawback is the limitation in pressure (15 bar with standard porous plates and air-water couple) leading to a minimum pore radius of ~0.05 micron. However, the measured values are in the domain of petroleum reservoir applications.

1 Introduction

In core analysis, MICP (Mercury Injection Capillary Pressure) is mainly used to derive the extend of the transition zone in the reservoir and the pore throat size distribution (ptsdt). MICP is fast and accurate. However, mercury is toxic and should be avoided when possible. The purpose of this paper is to describe a fast method to derive capillary pressure curves without the use of mercury. The apparatus and the procedure presented here were recently patented (French Patent BR104810 [1]).

Gas or oil displacing brine (drainage) in a porous plate setup leads to Pc (capillary pressure) curves similar to those obtained with injection of mercury, after rescaling with surface tension (Leverett J functions). Sabatier [2] presented a series of gas-brine experiments showing a good agreement between porous plates and mercury results, but significative differences with centrifugation measurements (even after Forbes corrections). Using oil-brine systems, Greder [3] found that oil-brine Pc were always greater than MICP curves, with differences in saturation up to 40% of pore volume. The difference was related to the amount of clay in sandstone samples.

Several studies have interpreted the difference between porous plates and MICP results by the loss of capillary continuity between the sample and the porous plate.

Good capillary continuity requires surfacing of the sample end faces with a grinding machine and applying high pressure on the sample to press it towards the porous plates. When these conditions are not satisfied, the injected fluid can invade the space between the sample and the porous plate. This mechanism is well described in the book written by McPhee *et al.* [4]. When pressure reaches a few bars, the Pc curve does not continue to follow its smooth shape but becomes nearly vertical (Figure 1). Similar results are described by Zubo [5] in a study of the establishment of irreducible saturation. In a study concerning the normalization of Pc curves, Desouky [6] presented a set of Pc curves that also illustrates this mechanism (Figure 2). The capillary contact was also discussed by Fleury [7].

* Corresponding author: roland.lenormand@cydarex.fr

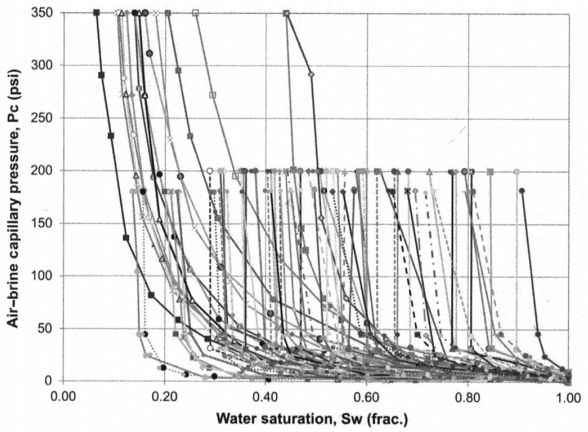

Fig. 1. Loss of capillary continuity between the plug and the porous plate (from [4].

The loss of continuity arises after a few bar pressures, corresponding to a meniscus radius of the order of the micron. The injected non-wetting fluid (gas or oil) can enter a space of this size between the plate and the sample. Since it is difficult to mill the surfaces with this accuracy, the standard procedure is to compensate the surface irregularities by placing a fine powder or a filter paper, but the grains of the powder are generally larger than one micron.

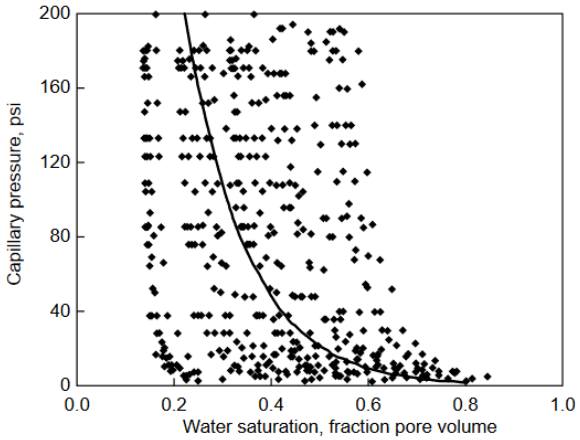

Fig. 2. Pc curves probably with loss of capillary continuity (after Desouky [6]).

Experiments with standard plugs of several centimeters take several weeks, sometimes several months when crude oil is used. Porous plate experiments can be easily simulated using a two-phase flow simulator such as CYDAR and the parameters that control the duration are the porous plate permeability at low pressure and the sample effective permeability near Swi. The duration is also proportional to the pore volume. One counter-intuitive result is that the duration is greater for high permeability (K) samples than for low, when the same porous plates are used. For high K samples, small pressure steps are required, and the production through the porous plates is proportional to the pressure gradient.

To reduce the duration, the first approach was to use Nuclepore and Millipore filtration membranes (respective thickness 6-11 and 150 microns), with less flow resistance than ceramic porous plates (Hammervold [8]). The samples were 5 cm long and the capillary pressures were limited to 1.5 bar. Longeron et al. [9] used a 2 cm long sample with lateral surface coated with low melting point metal alloy and studied different types of membrane. They were able to study complete cycle for wettability determination in around 2 weeks. The primary drainage was performed in around 1 week with capillary pressure limited at 1 bar and in 2 weeks with 2.5 bar maximum capillary pressure. Fleury [10] improved the method by using a rubber sleeve, which is more convenient to operate that the metal alloy and allowing the use of radial electrodes. However, at higher pressures, the gas passes through the membrane by molecular diffusion and the measurement of the displaced liquid is no longer possible.

Salehzadeh [11] also proposed an apparatus for measuring capillary pressure and relative permeability in unsaturated soils. He used disks of soil around 15 mm in thickness and 10 cm in diameter, with a porous membrane. The originality was to place two tensiometers along the sample to measure the pressure in water to derive the relative permeability together with Pc during transient steps by numerical history matching. With this apparatus, there was no problem of capillary contact since the soil is unconsolidated. The apparatus was limited to very low capillary pressures, below 0.1 bar.

Kokkedee [12] used a constant injection flow rate instead of a constant pressure difference in a standard core holder with water-wet and oil-wet porous plates. Analytical (assumption of small steps and linearization of the parameters) and numerical simulations were used to verify that the capillary equilibrium was reached. Relative permeabilities were obtained by combining constant rate out of equilibrium and stop to obtain a transient production. All the experiments were conducted below 1 bar.

Not waiting for complete stabilization at each step also reduces the duration. Fleury [13] introduced the FRIM (Fast Resistivity Index Method): several pressure steps are applied but without waiting for the equilibrium to be reached. The method is suitable for RI but not for capillary pressure. For capillary pressure, the standard method uses an extrapolation of the transient production effluent to derive the value at equilibrium. For instance, a sum of two exponential functions were introduced for centrifugation by King [14] and used by Fleury [15] Shafer [16] improved the method using a 4-parameter model.

In this paper, we show that we can reduce the duration of an experiment to around one day by improving the experimental set-up. The result is achieved by changing the design of the porous plate apparatus, using thinner samples, and using two porous plates of the same wettability to reduce the duration by a factor 2. The main result of our study is the possibility to determine the pore size distributions in a large range of permeabilities that agree with MICP values. The optimum duration, which is a compromise between speed and capillary equilibrium, is investigated using numerical simulations. Numerical simulations are used to control that the experiments are performed under acceptable equilibrium

conditions. We also show that it is possible to derive a Pc curve from an experiment performed without reaching equilibrium.

2 Experimental set-up

Our experimental set-up allows the determination of positive capillary pressure curves and the corresponding resistivity index. Measurements are performed at room temperature with 1" diameter samples, but the apparatus can be easily modified to work at higher temperature with larger diameters. There are two designs: one for small disks (3-6 mm) and 2-electrode resistivity measurements and one for 4-electrode measurements with longer samples (15 mm).

2.1 Apparatus for 2-electrode RI

The coreholder is shown in Figure 3 and Figure 4. This version is designed for short samples (3 -10 mm) with a 2-electrode resistivity index measurement. Its main specifications are the following:

- There is no confining pressure. Stress is not an important parameter for Pc and ptsd measurements (effect on permeability and porosity can be corrected using Leverett J-functions). The advantages are a faster installation of the plug and less equipment needed. In addition, the plug does not need to be circular since there is no lateral sealing on a rubber sleeve (often the case with Side Wall Cores). But the apparatus cannot be used for unconsolidated samples.
- The stress on the sample for a good capillary contact is provided by a spring inside the core holder, like in the old version of restored state measurements. The advantage is that the applied force is independent of the pore pressure at the opposite of a standard coreholder where the pore pressure acts against the confining pressure. The force on the spring is around 200 dN, leading to a pressure of 40 bar on a 1" sample. The capillary contact is better than with a rubber sleeve.

Fig. 3. Coreholder containing the 2 porous plates and the sample. The two outlet tubings are used to provide the electrical contacts.

- Two water-wet porous plates are used for faster production (factor 2) and better symmetrical electrical contact for RI measurements. We have used 15 and 3 bar air bubble pressure porous plates from Soil Moisture, thickness of 6 mm. The permeabilities of the plates are respectively 0.06 and 0.22 mD. Other porous plates with higher or lower entry pressures can be used. But high entry pressure plates have lower permeability.
- Electrodes are realized by stainless steel screens placed under the porous plate and in electrical contact with the tubing.
- Gas or oil are injected through lateral fittings.

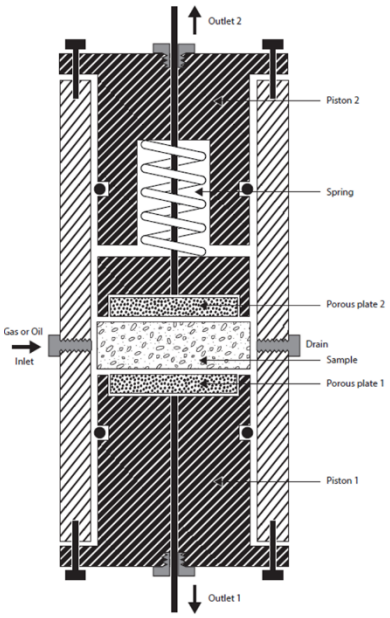

Fig. 4. Cell with the 2 porous plates designed for fast Pc measurement and the 2-electrode resistivity index. Length of the sample is under 1 cm.

2.2 Measurement of effluent volume

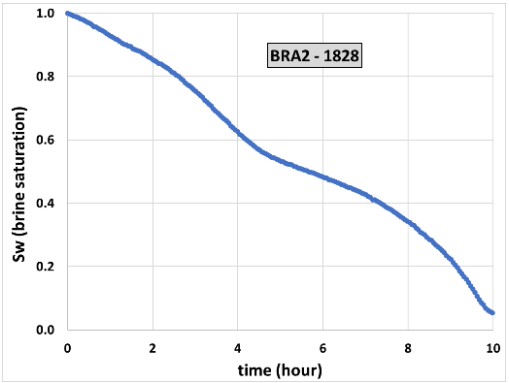

Fig. 5. Example of record of saturation using a balance.

The pore volume of the small disks is between 0.5 and 1 cc. We have tested the capacitive measurements described by Fleury and Doevle [17], and the increase of pressure in a small bellow equilibrated with a spring like in the measurement on cuttings with the DarcyLog apparatus (Lenormand [18]). Both methods are accurate, although it is difficult to avoid air trapping in the small diameter capacitance tube or in the bellow. We have found that the easiest method is to measure the weight using a standard balance. The outlet tube is immerged in a beaker to avoid the discontinuity of drops with a small amount of viscous oil on the surface to avoid water evaporation. Using a balance with a +/- 2 mg accuracy,

the saturation is determined with around 1 SU accuracy (Saturation Unit). An example of record of saturation derived from the balance is shown in Figure 5. For quality control, the final saturation is determined by weighing the sample at end of experiment.

2.3 Apparatus for 4-electrode RI measurement

A similar but longer coreholder is used for 4-electrode measurements with a support for 2 potential electrodes around the sample (Figure 6). In this case, the sample must be longer (15 mm) and roughly circular. The current electrodes (E1 and E2) are connected through the porous plates. The potential electrodes are made of stainless-steel springs that can move inside a groove. The spring voltage is recovered through a brass ring in this support and isolated taps (E2 and E3) mounted on the coreholder allow the connection to a voltmeter.

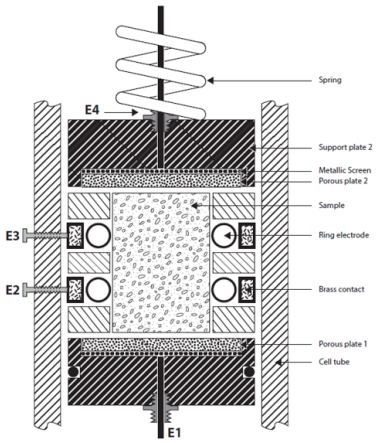

Fig. 6. 4-electrode cell. The length of the sample is 1.5 cm. Like for the2-electrode cell, air or oil is injected laterally (fittings not represented on this diagram)

2.4 Principle of the measurements

The set-up is shown in Figure 7. The sample and the porous plates are saturated with brine under vacuum and 20 bar pressure is applied for several hours then placed in the core holder. The resistances of the porous plates and the plugs are measured separately before mounting them in the cell to make resistance corrections since the resistances of the plates are not negligible (resistances in series with the resistance of the plug). Standard lab equipment operating at 1000 Hz is used for the resistivity measurements.

The cell is closed with bolts to compress the spring. The apparatus allows injection of either oil or air. When oil is used, oil is injected at low pressure through one lateral fitting and air in the cell is evacuated by the other fitting.

For ptsd, it is necessary to have a continuous or very small-step injection, like for MICP. Constant flow rates[12] were tested but because flow rate must be lower at the end of experiment to allow the capillary equilibrium, the duration of the experiment was not optimum. Instead, we use a continuously increase of pressure, with a lower increase at the beginning of the experiment to allow the desaturation of the plateau. This pressure ramp is obtained by injecting a liquid at constant flow rate in the buffer vessel. Figure 8 shows the record of the pressure for durations of 1, 10 and 20 hours. If necessary, other forms of pressure functions can be imposed using a computer-controlled pump, or a system of controlled electro-valves.

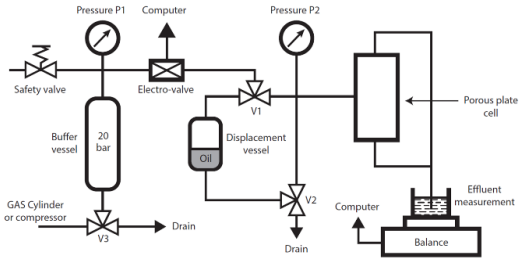

Fig. 7. Experimental set-up for gas or oil injection.

Like in MICP, water is displaced from the surface of the plug before continuous invasion in all the sample (conformance effect as described by McAPhee [4] also called closure correction, fig. 9.34 in the book). The determination of the entry pressure is important for porosity determination but have a limited impact on ptsd. With our equipment, the simultaneous measurement of the resistivity allows a better determination of the entry pressure point, since the resistivity starts to increase when gas (or oil) enters the sample. In addition, the plot of RI as a function of saturation in a log-log scale is always near linear with a slope close to 2, therefore the entry point can be determined with accuracy.

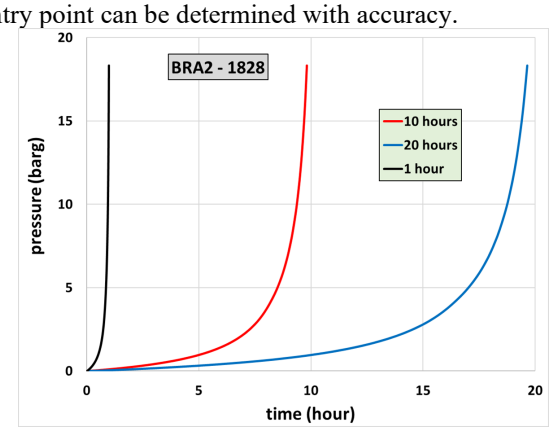

Fig. 8. Example of injection pressures as function of time.

The capillary pressure curve (Figure 9) is derived from the pressure and effluent mass records and the standard incremental logarithmic distribution (ptsd) is calculated the same way as for MICP (Lenormand [19]).

Before and at end of the experiment, the disk is weighed to determine the porosity and the final saturation. The accuracy of the porosity measurement proves that there was no evaporation during the few minutes of measurement.

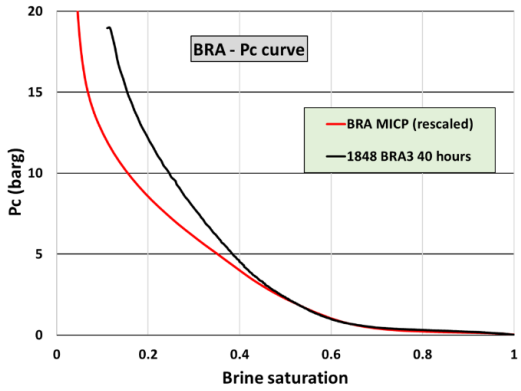

Fig. 9. Example of Capillary pressure curves determined experimentally from the injected pressure and the effluent production.

3 Results

We will first present results with step pressure injection, drainage, and imbibition curves and 2- and 4-electrode resistivity index. The rest of the paper will be devoted to the determination of the ptsd and the comparison with MICP.

3.1 Drainage and imbibition capillary pressure (step pressure).

With the 4-electrode cell (15 mm samples), we performed standard oil-brine experiments with pressure steps and waiting for equilibrium. Figure 10 shows the injected oil pressure and average oil saturation in the sample as a function of time. Drainage and imbibition took around 3 days each. The corresponding capillary pressure curves in positive drainage and imbibition are shown in Figure 11.

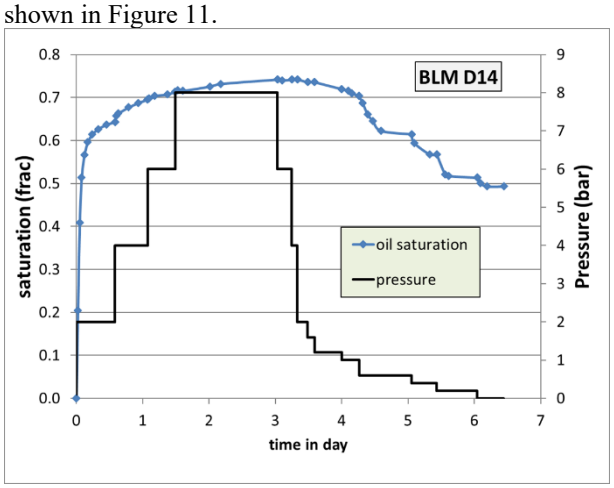

Fig. 10. D14: Example of step injection for drainage and imbibition.

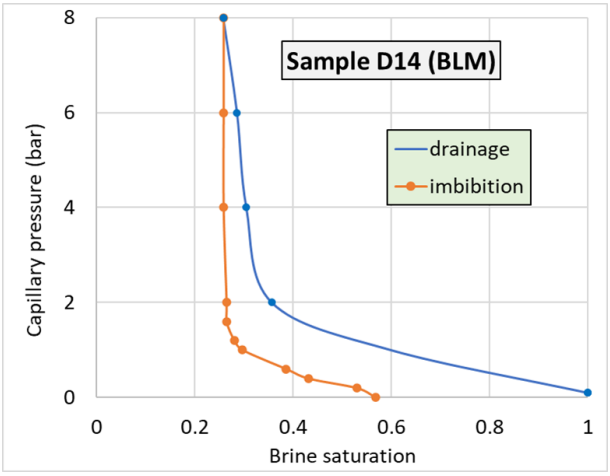

Fig. 11. D14: Drainage and imbibition Pc curves from step injection.

3.2 Resistivity index: 2-Electrode vs. 4-Electrode methods

Figure 12 shows the resistivity index measured with the 2- and 4-electrode methods with oil on a 15 mm BRA sample. All measurements show an excellent agreement between the 2- and 4-electrode measurements.

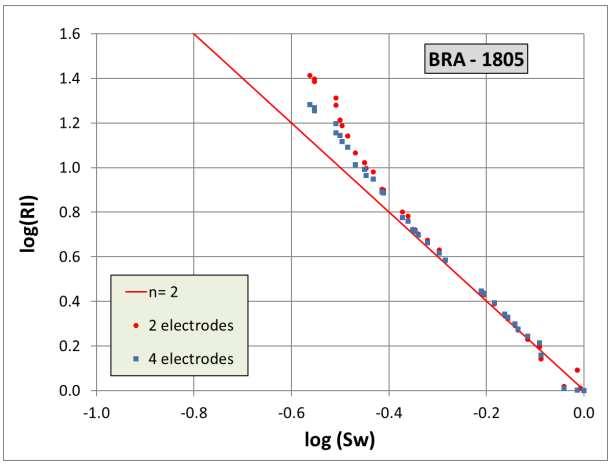

Fig. 12. Example of Resistivity Index using both 2- and 4-electrode methods during a drainage experiment.

3.3 Pore throat size distribution

Table 1. Properties of the samples used for comparison with MICP.

sample	Porosity (frac)	Permeability (mD)	comments
BLM	0.20	6	brick
BRA	0.25	100	carbonate with double porosity
GM	0.13	0.05	sandstone
LAV-A	0.15	2	carbonate with double porosity
GV	0.20	1000	sandstone with clay
BEN	0.20	1000	sandstone

The method was tested on several samples with a large range of permeabilities (Table 1) and compared to MICP

results. For all the samples, the thickness of the disks is around 6 mm. The samples used for the porous plate and MICP come from the same block, but we did not perform the MICP directly on the samples used with the porous plates; consequently, small differences in the properties are always possible. MICP measurements were performed by service companies.

We are not expecting the exact same results for air and mercury since the wettability properties and the pressures are different. All air porous plate experiments were interpreted using 70 dyne/cm (0.070 N/m) and a zero-contact angle. There were no adjustable parameters. The 15-bar bubble pressure porous plates are used for most of the samples. 3 bar bubble pressure were used for BEN and GV that have large permeabilities.

- BRA (Figure 13): Brauvillier carbonate. The double porosity is well determined on the porous plate like in MICP.
- BLM (Figure 14): Red construction brick. A small contribution of a double porosity under 1 micron pore size is observed on the MICP and the slow displacement (20 hours) but not on the fast displacement (10 hours) due to the lack of capillary equilibrium.
- GM (Figure 15): Molieres sandstone. There is a good agreement with MICP, but there is no measurement below 0.1 micron with porous plates (due to the capillary pressure limited at 15 bar).
- LAV-A (Figure 16): Lavoux carbonate. The double porosity is observed in both MICP and porous plate. This double porosity is observed on smaller radius than BRA sample.
- GV (Figure 17): Red Vosges Sandstone. Good agreement between MICP and Porous plates. The porous plate can easily characterize pores of 100 microns corresponding to an injection pressure of 100 mbar.
- BEN (Figure 18): Bentheimer sample. The agreement is not very good. BEN is a sample with high permeability and high porosity. We also observed discrepencies between MICP results coming from two different laboratories (curves MICP 1 and 2). It is possible that the error comes from the MICP, which could be run too fast for the low pressure and high pore volume, as discussed in Maas [20].

Figure 19 shows the two extreme cases on ptsd measurements, with the large range of measurements between 0.1 and 100 microns.

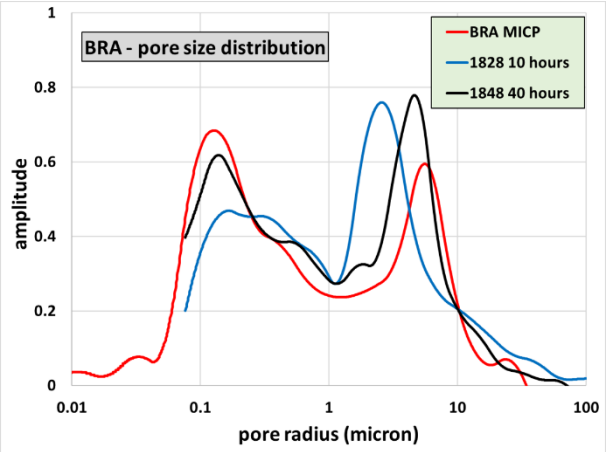

Fig. 13. BRA sample: ptsd determined with the porous plate method for two different durations of experiments compared to MICP result.

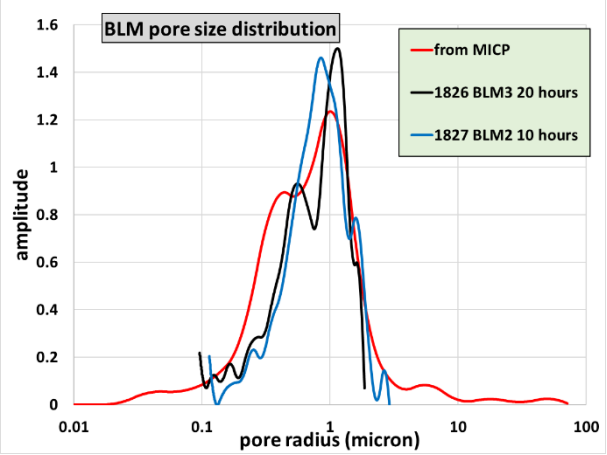

Fig. 14. BLM sample: ptsd determined with the porous plate method for two different durations of experiments compared to MICP result.

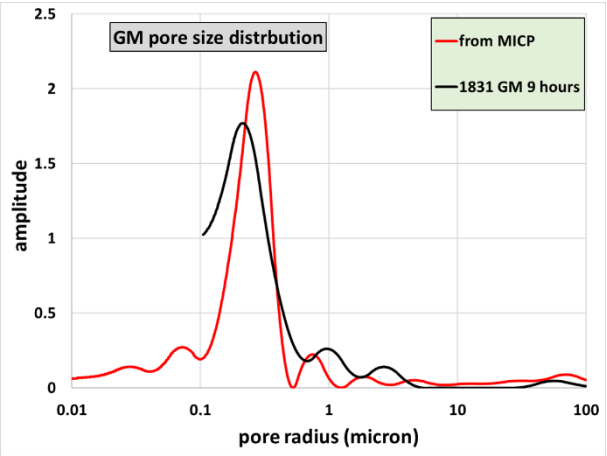

Fig. 15. GM sample: ptsd determined with the porous plate method compared to MICP result.

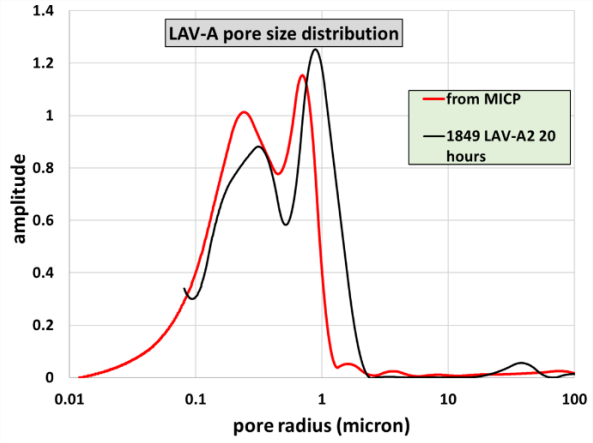

Fig. 16. LAV-A sample: ptsd determined with the porous plate method compared to MICP result.

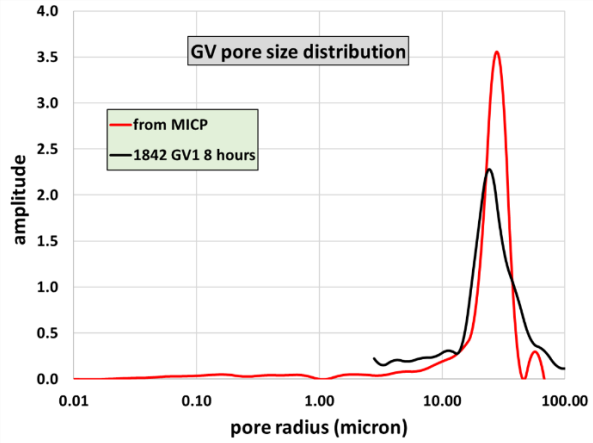

Fig. 17. GV sample: ptsd determined with the porous plate method compared to MICP result. This experiment is performed with the 3 bar entry pressure porous plates.

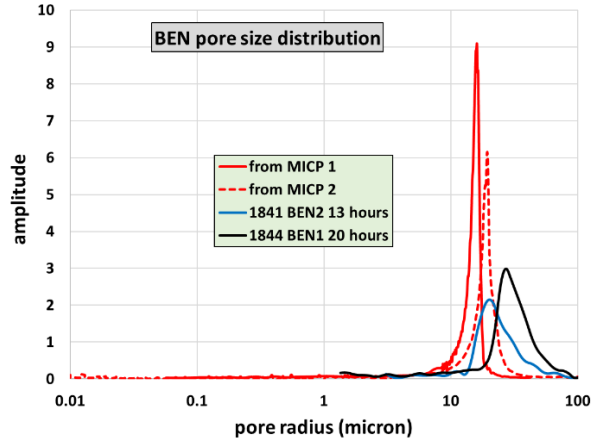

Fig. 18. BEN sample: ptsd determined with the porous plate method for two different durations of experiments compared to two MICP results (two different companies). These experiments are performed with the 3 bar entry pressure porous plates.

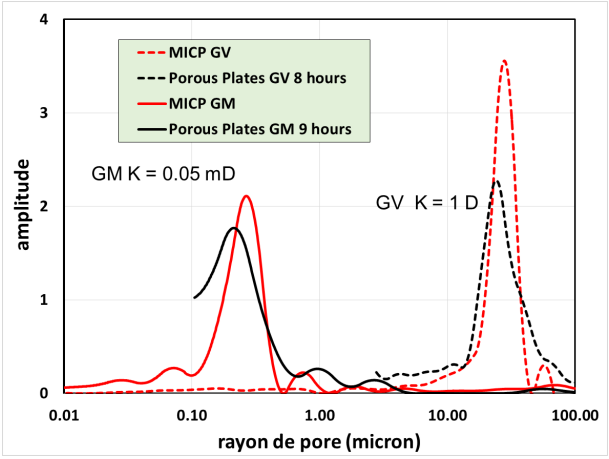

Fig. 19. The two extreme cases in terms of pore size showing the interval of the possible measurements from 0.1 to 100 microns.

4 Discussion

To determine the optimum duration of measurements, we have studied numerically the effect of the various parameters on the double porosity BRA sample. The double porosity allows a good understanding of the effects of the various parameters on small or large pore parts of the ptsd curve. However, this example with 25% porosity cannot be generalized to all the samples. A similar study with unimodal and lower porosity BLM is given in the last part of this section to establish an optimum duration diagram.

The numerical simulations are performed using the commercial software CYDAR, with the MICP Pc curve as "reference Pc" curve and a standard Corey set of relative permeabilities as input. Saturation is derived from the effluent production and the "apparent" capillary pressure curve is then optimized. Then the ptsd is calculated and compared to the initial MICP curve. The length of the sample is kept equal to 6 mm which is the minimum size to obtain a good accuracy on saturation determination. The simulation is 1-dimentional, performed on one half of the sample (symmetrical conditions for flow).

4.1 Effect of the duration of injection

Figure 20 shows the effect of duration with a low permeability porous plate (0.01 mD). For this case, 100 hours are necessary to have a ptsd similar to the MICP distribution (Reference Pc in Figure 19). For all simulations, the difference between MICP (reference Pc) and porous plates is seen only at large pores, when the flow is controlled by the permeability of the porous plate. The smallest pores, between 0.1 and 1 micron, are determined by the flow controlled by the effective permeability of the sample, not affected by the low permeability of the porous plates.

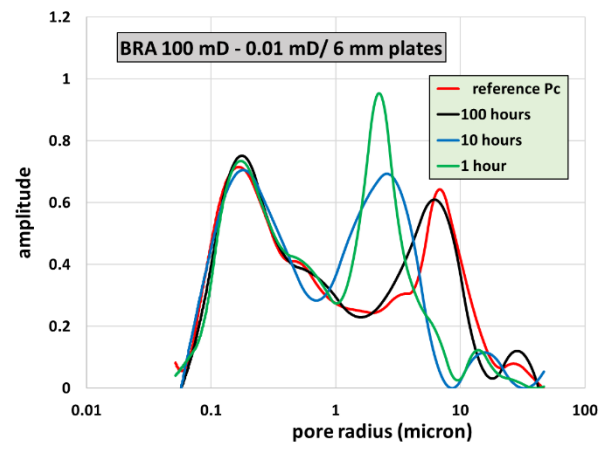

Fig. 20. Numerical simulations: effect of the duration of injection.

4.2 Effect of injected fluid viscosity

Figure 21 shows the result for gas and two types of oil (1 and 40 cP viscosities) injected for 25 hours with porous plates of 0.1 mD permeability. The viscous effect only concerns the beginning of the displacement (large pores, low Pc). There is very little difference between the gas and low viscosity oil; the kinetics being mainly controlled by the flow of water through the porous plates. These two experiments are close to the reference curve and can be considered as acceptable. For the high viscosity oil, the viscous effect is more important, and the flow rate should be reduced.

There is no effect of viscosity on the small pore part of the curve, since the flow is controlled by the water relative permeability of the sample. In this domain, the relative permeability of the injected fluid is close to unity.

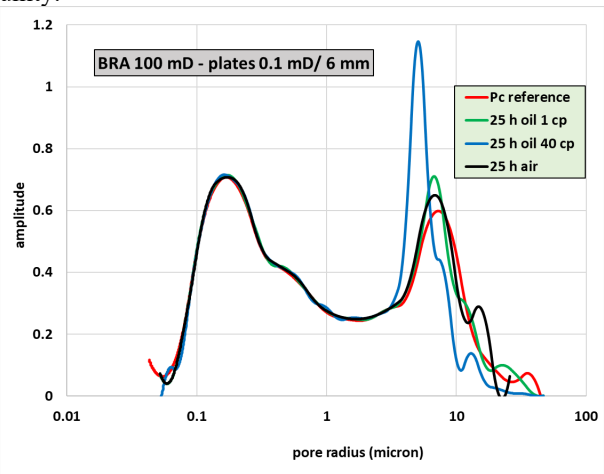

Fig. 21. Numerical simulations: Effect of the viscosity of the injected fluid: gas and oil.

4.3 Effect of the permeability of the porous plate

We have studied the permeability of the porous plate required for an experiment duration of 1 hour (air injected). Figure 22 shows that the permeability of the porous plates should be larger than 1 mD, a result difficult to obtain with standard plates (our plates have permeability around 0.05 mD). For other durations, the results are displayed in the diagram that summarizes the results (Figure 23).

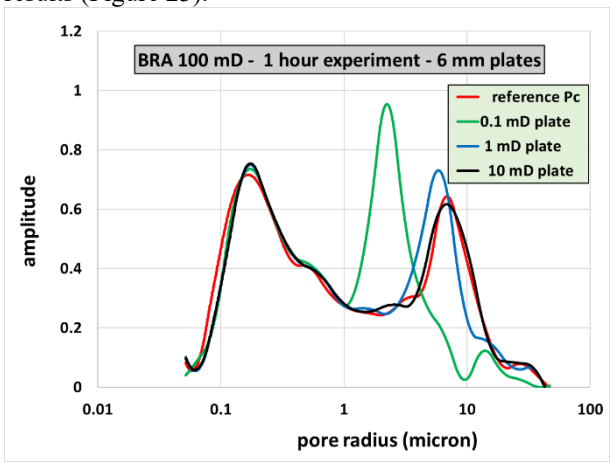

Fig. 22. Numerical simulations: effect of the permeability of the porous plates.

4.4 Optimum Duration Diagram for BRA

We have also studied the effect of sample permeability, assuming the same shape for the ptsd and an effect on the capillary pressure using the J Leverett function (capillary pressure scaled with the squared root of the permeability). The porous plates are characterized by the ratio of the permeability over its thickness K/e, which controls the pressure drop. This diagram is calculated for air injection and BRA type of sample with 25% porosity.

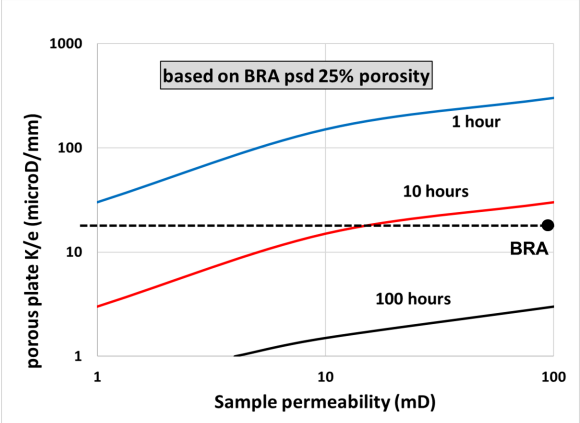

Fig. 23. Diagram used to estimate the optimum duration. The numerical simulations are based on the ptsd of the Brauvillier limestone (BRA), with a porosity of 25%. Our apparatus with the 15 bar porous plates (dashed line) allows measurements on this type of sample in less than 10 hours when its permeability is below 20 mD. For the BRA sample (black dot) the optimum time is around 20 hours.

The results of the numerical simulations are summarized in the Figure 23. The lines are the optimum durations to obtain a ptsd close to the MICP result. The horizontal dashed line corresponds to our experimental set-up. For the BRA sample used in our experiments with 100 mD permeability (black dot), the diagram gives an optimum duration around 20 hours, in agreement with the experimental results.

This diagram is established for BRA and is not universal; it depends on the form of the ptsd curve and the porosity. Similar simulations can be performed for other samples. For low permeability and low porosity samples like GM, the optimum duration is shorter. The results are presented below.

4.5 Effect of porosity

With all other parameters kept the same, the duration of a displacement is proportional to the pore volume of the sample. All the simulations are performed with the 25% porosity, we present below results for other samples with lower porosity.

4.6 Optimum duration for unimodal porosity samples

We have performed numerical simulations for other samples than BRA, based on a unimodal distribution and the BLM ptsd with 20% porosity. Like for BRA, the effect of permeability on the Pc curve is derived from the J Leverett function. With the 15 bar porous plates, experiments can be performed in less than 20 hours for permeabilities below 200mD and less than 5 hours below 100 mD (Figure 24).

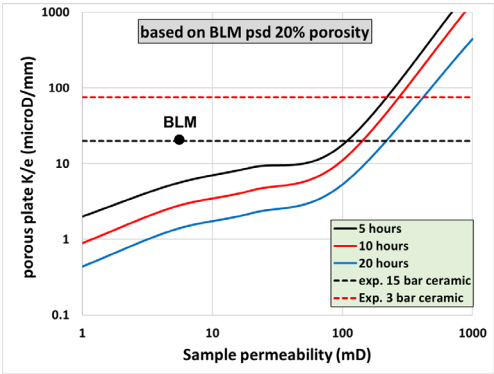

Fig. 24. Optimum duration for a sample with unimodal and 20% porosity based on BLM ptsd. The black dashed line corresponds to the apparatus with the 15 bar porous plates and the red line to the 3 bar porous plates. The black dot corresponds to the experiment: the conclusion is that the experiment could be run faster than 5 hours.

Figure 25 shows the diagram based on the Bentheimer (BEN) unimodal ptsd with the 15 bar porous plates. The red dots correspond to the GM and GV samples. The 20 hours limit is only reached for samples with permeability larger than 1 D and porosity larger than 35%, which is quite unusual for reservoir samples.

4.7 Quality control

Maas[20] has shown that during MICP measurements, the ptsd is strongly dependent on the equilibration time. Using standard procedure for duration of steps can lead to error in saturation as large as 0.20 (from 0.2 to 0.4 for instance). This error has an impact for the estimation of the transition zones. The conclusion of Mass paper is the recommendation to use a two-phase numerical simulator to verify that the capillary equilibrium is reached during the experiment. We follow the same procedure, since the problem of equilibrium is more critical with porous plates than with mercury. In addition to the effect of relative permeability inside the sample at high pressure, there is a monophasic flow inside the porous plates at low pressure that slow down the production at low pressure.

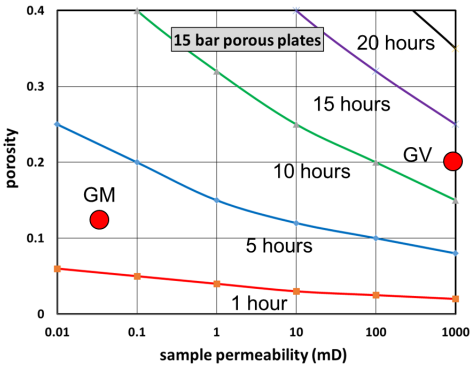

Fig. 25. Diagram used to estimate the optimum duration. The numerical simulations are based on the ptsd of the BEN sandstone with the 15 bar plates.

In the previous parts of the discussion, we have compared the measured ptsd to the one determined by MICP. However, for a real experiment, we do not have the MICP result. The method for quality control is shown in Figure 26, with BLM, a sample with intermediate permeability (5 mD). The experimental Pc curve is introduced in the numerical simulator (module Porous Plates of the simulator CYDAR), with a standard set of Kr. The simulation is run using the recorded injection pressure as input. Effluent production (in red, Figure 26) is then derived from the calculated production and compared to the experimental one (in blue). With perfect equilibrium during the experiment, the two curves should be superimposed. The differences between the two curves are used to quantify the error, and a criterium for quality control can be imposed.

This BLM experiment (Figure 26) can be interpreted in several domains:

- Under 4.5 hours, this portion of the curve can be considered as the conformance: water on the surface and invasion in the largest pores on a limited distance from the surface. During this production, pressure is rising slowly but the displaced volume is small, consequently equilibrium is reached.
- Between 4.5 and 8 hours, the production corresponds to the "plateau" of the Pc curve, with a small increase of pressure but a large volume of water displaced. At a given time the simulated production (in red) is lower than the experimental value (in blue), showing that the equilibrium is not perfectly reached. The limitation is mainly due to the porous plate.
- Over 8 hours, the pressure increases quickly, and the displaced volume is small. The equilibrium is reached.

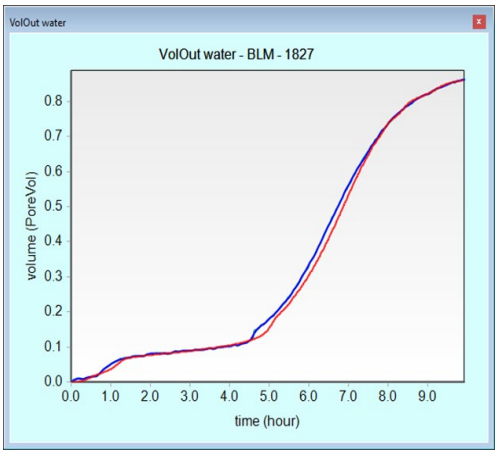

Fig. 26. Experiment 1827 on BLM sample: effluent production as function of time. In blue the experimental curve and in red the numerical simulation.

Figure 27 presents a similar study on BRA sample: the experimental saturation in blue is compared to the simulated one (in red). The difference at low pressure is due to the porous plate. For BRA, porosity is larger and Pc lower than BLM. Consequently, it takes more time to displace water at the beginning of the experiment and this part of the curve (less than_5 hr) is not in equilibrium.

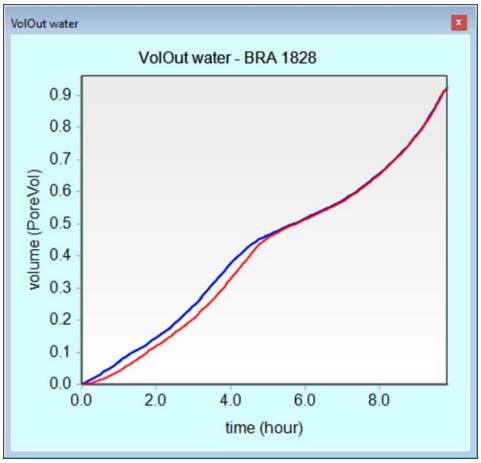

Fig. 27. Experiment 1828 on BRA sample for 10 hours. Experimental production in blue and numerical simulation in red. The conclusion is that the experiment can be considered as acceptable.

Figure 28 presents the result for BEN sample: the experimental saturation in blue is compared to the simulated one (in red). The difference comes from the plateau of the Pc curve, large volume to be displaced at low pressure.

5 Dynamic correction

The numerical simulations can be used to determine the true "equilibrium" Pc curve from an experiment not at equilibrium. This method was already used by Salehzadeh [11] and Kokkedee [12] for optimization on the Pc and Kr curves. Mass [20] discussed the numerical simulations to control the equilibrium during MICP experiments but did not propose numerical optimization for correction.

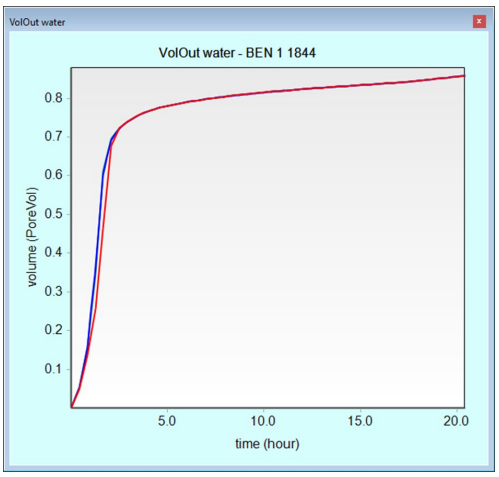

Fig. 28. Experiment 1844 on BEN-1 sample for 20 hours. Experimental production in blue and numerical simulation in red. The conclusion is that the experiment can be considered s acceptable.

Figure 26 shows the difference between the experimental and the simulated water production using the Pc curve calculated experimentally. Then this Pc curve is optimized to find the optimal fit between experimental and simulated production. The result for the optimized Pc curve is shown in red in Figure 29. For a given capillary pressure, the water saturation is lower on the optimized Pc curve since the equilibrium is supposed to have taken place (more time for production). The "equilibrium" pore throat size distribution is then calculated using this optimized Pc curve. Figure 30 shows the experimental distribution in blue and the new equilibrium one in red.

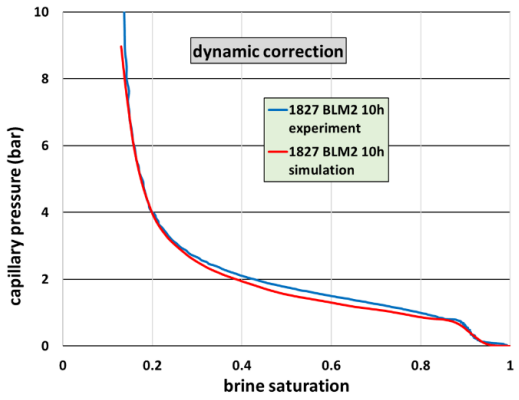

Fig. 29. BLM 1827: experimental determination of the capillary pressure (in blue) and Pc corrected using numerical optimization (in red).

So far, we have not investigated experimentally the possibility to derive the "true" ptsd distribution (obtained in equilibrium conditions) from an experiment performed out of equilibrium. This numerical correction may reduce the duration to a few hours and will be studied in the future. But the mathematical tools are available in the software CYDAR, using optimization

with splines functions with more than 20 nodes, to retain the details of the shape of the Pc curve.

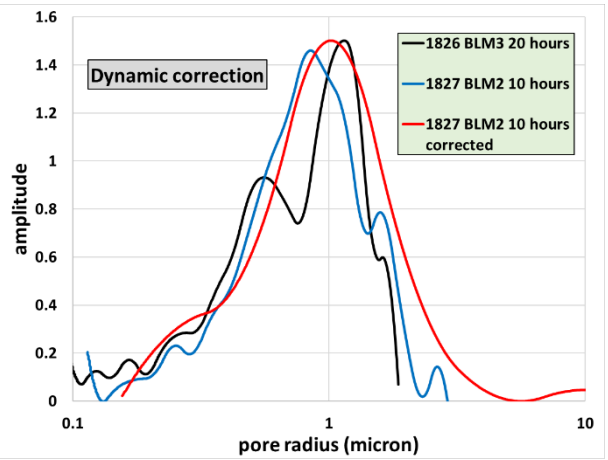

Fig. 30. Ptsd using the numerical correction (in red).

6 Application for replacement of MICP measurements

Our method allowing quick measurement of the Pc curve that can replace MICP for reservoir applications: determination of transition zones, quick estimations of permeability using Swanson-type correlation, and pore throat size distributions.

- For capillary pressures with a maximum pressure at 15 bar, the determination can be performed in less than one day. This is generally longer than MICP measurements which takes a few hours. However, the equipment is less expensive, do not require toxic mercury, and since the measurement is fully automatic, several measurements can be run at the same time. The time for preparation of the sample is similar in the two methods.
- Other types of porous plates can be chosen for higher capillary pressure, up to 100 bar using membranes or VYCOR plates. But with such plates, the duration of the measurement will be longer (Shafer and Lasswell [16]).
- The main advantage of our apparatus is safety and environmental concern since the couple water/air or water/oil is used instead of vacuum/mercury.
- Generally, the drainage Pc and ptsd are determined on the trim ends of the plugs (either 1" or 1.5") after Soxhlet cleaning. From our experience, it is more accurate to determine the porosity directly before the porous plate measurement since the entry point is never well defined (conformance). Porosity is determined without additional measurements, from the difference of mass between the saturated and dry disk, using either the grain density or the geometric volume.
- In addition, the permeability can be determined directly with a good accuracy, better than the standard correlations (Swanson) using either the DarcyPress method [21], or a direct surface measurement on the disk with a guard ring [22].

7 Concluding Remarks

The main purpose of this study is to present a new device allowing faster and reliable porous plate experiments for resistivity index and capillary pressure determinations.

7.1 Apparatus

- We have described a porous plate apparatus allowing faster experiments than standard equipment. The main improvements are the following:
- Design without a rubber sleeve for confining pressure, allowing faster mounting and possibility of non-circular samples (broken plugs or side wall cores).
- Use of two water-wet porous plates, to double the effluent production and to provide a symmetrical efficient electrical contact.
- Use of thin samples with small pore volume but with accurate production measurement using a balance. The study was realized with a 2 mg accuracy balance. A more accurate balance (0.1 mg) allows the use of thinner disks (2-3 mm).
- Use of a spring placed inside the coreholder to press the sample on the porous plate improves the capillary contact. The applied force is independent of pore pressure.
- For 4-electrode measurements, the potential electrodes are made of soft rings in stainless steel placed in grooves inside an isolated support.
- The apparatus is designed for positive capillary pressure since the main purpose is pore throat size distribution measurements, but negative values could be obtained using hydrophobic porous plates (but electrical measurements would not be possible). The apparatus uses 1" diameter samples, but the same type of apparatus can be designed for larger diameters.

7.2 Resistivity index measurements:

- 4-electrode measurements with oil or gas can be performed on 15 mm long sample in a few days.
- The improved contact with the high-force spring suppresses the so-called "contact resistance" and allows reliable 2-electrode measurements of the resistivity index, similar to the result obtained with the 4-electrode method. The main consequence is that thinner samples (6 mm) can be used, since there is no need to place longitudinal or radial electrodes on the sample.

7.3 Capillary pressure and pore throat size distribution

- Like for MICP, the pore throat size distribution can be calculated from the gas or oil capillary pressure.
- Ptsd can be obtained in less than 24 hours with 15 bar bubble pressure porous plates. For high permeability (> 500 mD), more permeable porous plates with 3 bar bubble pressure can be used to reduce the duration.
- For most of samples, the pdst agree with MICP.

- Using numerical simulations, we have studied the effect of the various parameter on the optimum duration and calculated a diagram giving the optimum duration as a function of sample and porous plate properties.
- For quality control, we have proposed a numerical calculation to verify that the experiment is run under conditions close to equilibrium. We have given an example of a numerical optimization to determine the "true" Pc curve using an experiment performed out of equilibrium. This optimization could be used to reduce the duration of the experiments.
- With our equipment with 15 bar bubble pressure porous plates, the pore throat cannot be determined below 0.05 micron. However, the range of pore sizes and corresponding capillary pressures (15 bar) measured with our apparatus is in the domain of reservoir applications.
- From the shape of the Pc curve and the pstd, we can easily determine the point where the injected fluid starts to invade the porous plates. The interpretation is only valid before this entry pressure.
- Like for MICP, the results also allow the determination of transition zones, or the quick estimation of permeability for sample selection in SCAL program.
- All this study is performed on quarry samples which are all water-wet. For reservoir samples, the disks should be cleaned in Soxhlet to restore water wettability. The application of our method for reservoir samples will be tested in a future study.

References

1 French patent FM103935 19-07-29, dispositive pour mesurer des caractéristiques physiques d'un échantillon de solide.

2 L. Sabatier, Comparative study of drainage capillary pressure measurements using different techniques and for different fluid systems, SCA-9424, (1994).

3 H.N. Greder, V. Gallato, Ph. Cordelier, D. Laran, V. Munoz, O. d'Abrigeon, Forty comparisons of mercury injection data with oil/water capillary pressure measurements by the porous plate technique, SCA-9710, (1971).

4 C. McPhee, J. Reed and I. Zubizarreta, Core analysis: a best practice guide, Developments in Petroleum sciences, vol 64, Elsevier, (2015).

5 Z. Zubo, Luo Manli, ChenXu, Lv Weifeng, An experimental study of irreducible water saturation establishment, SCA2014-070, (2014).

6 S.E.D.M. Dezouky, A new method for normalization of capillary pressure curves, Oil and Gas Science and technology, Vol. 58,n° 5, pp 551-55, (2003).

7 M. Fleury, The spinning porous plate (SPP) method: a new technique for setting irreducible water saturation on cores samples, SCA2009-08

8 W.L. Hammervold, S.M. Skjaeveland, Improvement of diaphragm method for drainage capillary pressure measurement with micropore membrane, SCA1992-05EURO, (1992).

9 D. Longeron, W. Hammervold and M. Skaeveland, Water-oil capillary pressure and wettability measurements using micropore membrane technique, SCA-9426, (1994).

10 M. Fleury and D. Longeron, Combined resistivity and capillary pressure measurements using micropore membrane technique, SCA-9615, (1996).

11 A. Salehzadeh and A.F. Demond, Apparatus for the rapid automated measurement of unsaturated soil transport properties, Water Resources Research, vol. 30, n° 10, pp 2679-2690, (1994).

12 J.A. Kokkedee and V.K. Boutkan, Towards measurements of capillary pressure and relative permeability at representative wettability, EAGE conference, Moscow, (1993).

13 M. Fleury, FRIM: a fast resistivity index measurement method, SCA 9829, (1998).

14 M.J. King, K.R. Narayanan and A.J. Falzone, Advances in centrifuge methodology for core analysis, SCA paper 9011, (1990).

15 M. Fleury, P. Egermann and E. Goglin, A model of capillary equilibrium for the centrifuge technique, SCA2000-31, (2000).

16 J. Shafer and P. Lasswell, Modeling porous plate capillary pressure production data: shortening test duration and controlling data, SPWLA, (2007).

17 M. Fleury, M. Doevle and D. Longeron, Full imbibition capillary pressure measurements on preserved samples using the micropore membrane technique, SCA 1997-16, (1997).

18 R. Lenormand and O. Fonta, Advances in Measuring Porosity and Permeability on drill cuttings, SPE 111286, (2007).

19 R. Lenormand, Interpretation of mercury injection curves to derive pore size distribution, SCA2003-52, (2003).

20 J. Maas, N. Springer and A Hebing, Relative permeability effects overlooked in MICP measurements. Transition zones likely to be smaller, SCA2016-013, (2016).

21 R. Lenormand, F. Bauget, G. Ringot: Permeability measurement on small rock samples, SCA2010-32, (2010).

22 Yang, K.a, Basheer, P.A.M.a, Bai, Yb., Magee, Bc. and Long, A.E.: Assessment of the effectiveness of the guard ring in 1 obtaining a uni-directional flow in an in-situ water permeability test, Materials and Structures, 48 (1). pp. 167-183. ISSN 1359-5997, (2015).